Electronic Supplementary Information

Molecular Engineering of Complexation Between RNA and Biodegradable Cationic Gemini Surfactants: Role of the Hydrophobic Chain Length

Mohd. Akram[1,*], Hira Lal[1], Sonam Shakya[1], Rohit Varshney[2], Kabir-ud-Din[3]

[1]*Department of Chemistry, Aligarh Muslim University, Aligarh, India-202002*

[2]*Habitat Centre, Institute of Nano Science and Technology, Phase-10, Sector-64, Mohali, Punjab, India-160062*

[3]*Department of Chemistry, College of Natural and Computational Sciences, Arba Minch University, Arba Minch, Ethiopia*

*Corresponding author.

E-mail address: drmohdakram@rediffmail.com (M. Akram)

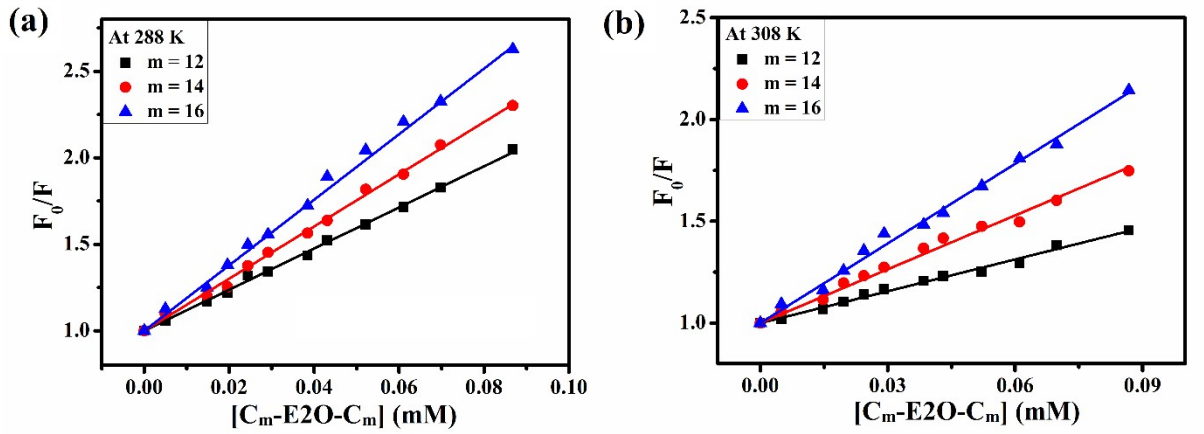

Figure S1. Stern-Volmer plots for quenching of intrinsic fluorescence of EB-RNA complexes in the presence of C_m-E2O-C_m gemini surfactants (m = 12, 14 and 16) in Tris-HCl buffer (pH = 7.4) at (a) 288 K and (b) 308 K.

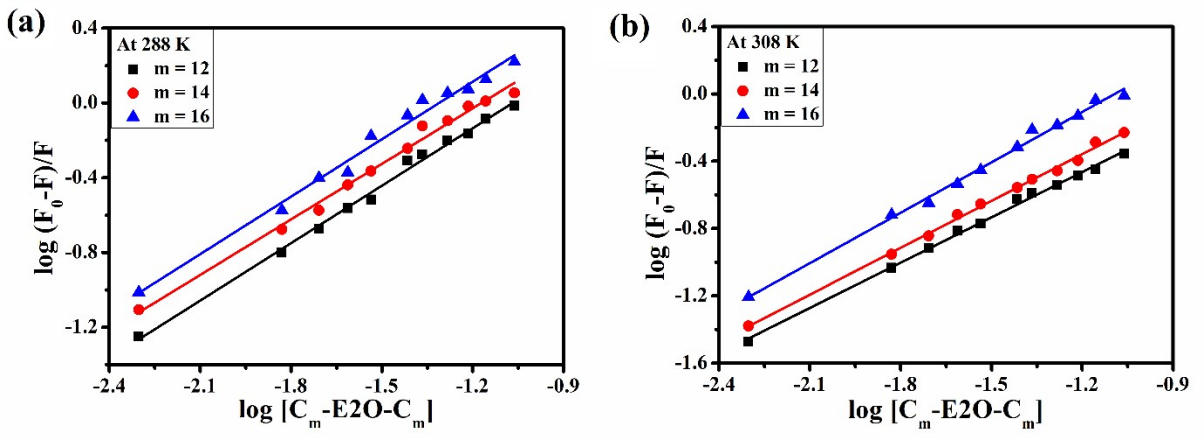

Figure S2. Modern Stern-Volmer plots for quenching of intrinsic fluorescence of EB-RNA complex in the presence of C_m-E2O-C_m gemini surfactants (m = 12, 14 and 16) in Tris-HCl buffer (pH = 7.4) at (a) 288 K and (b) 308 K.

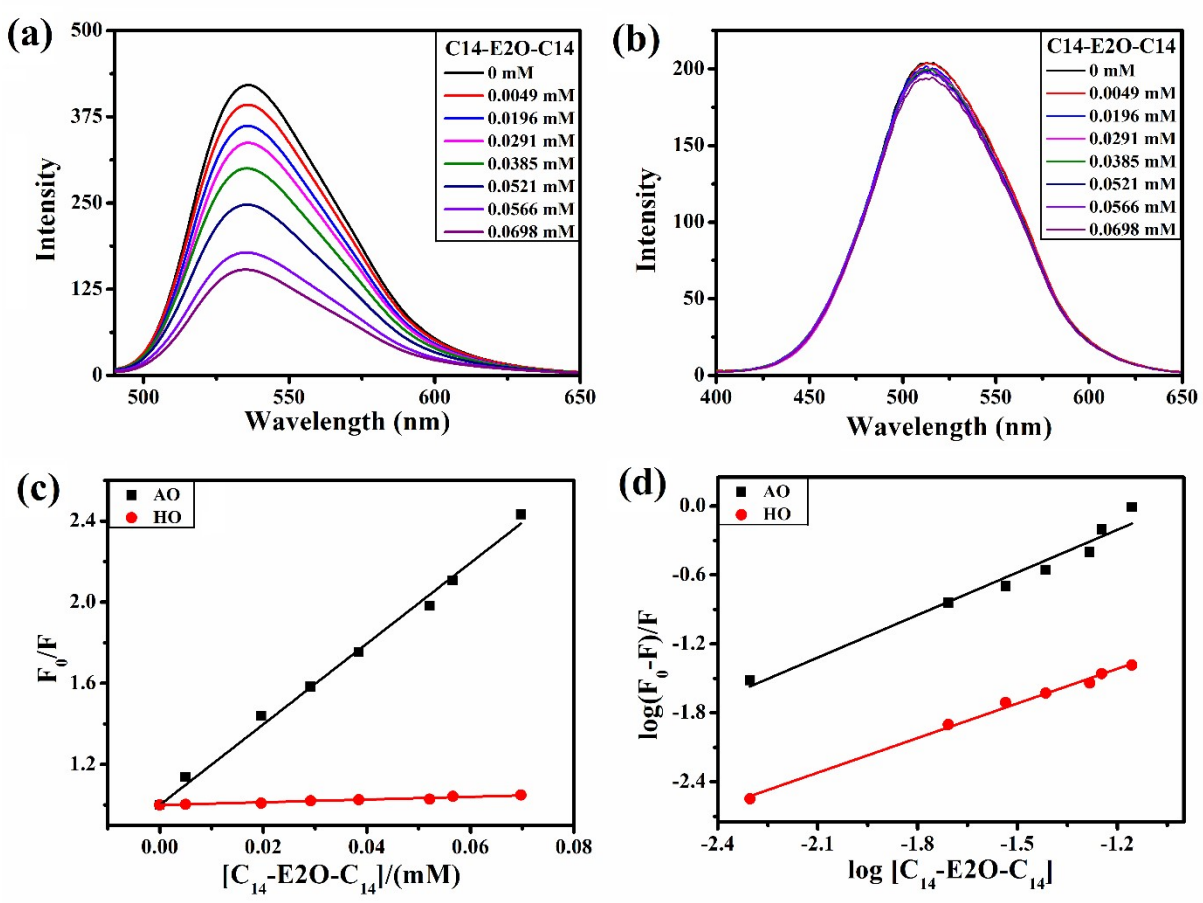

Figure S3. Competitive displacement assays between C_{14}-E2O-C_{14} gemini surfactant and dyes. Fluorescence titration of (a) AO+RNA and (b) HO+RNA systems with varying concentrations of C_{14}-E2O-C_{14} gemini surfactant. The respective Stern-Volmer and modern Stern-Volmer plots are shown in (c) and (d) (conditions: pH = 7.4, T = 298 K).

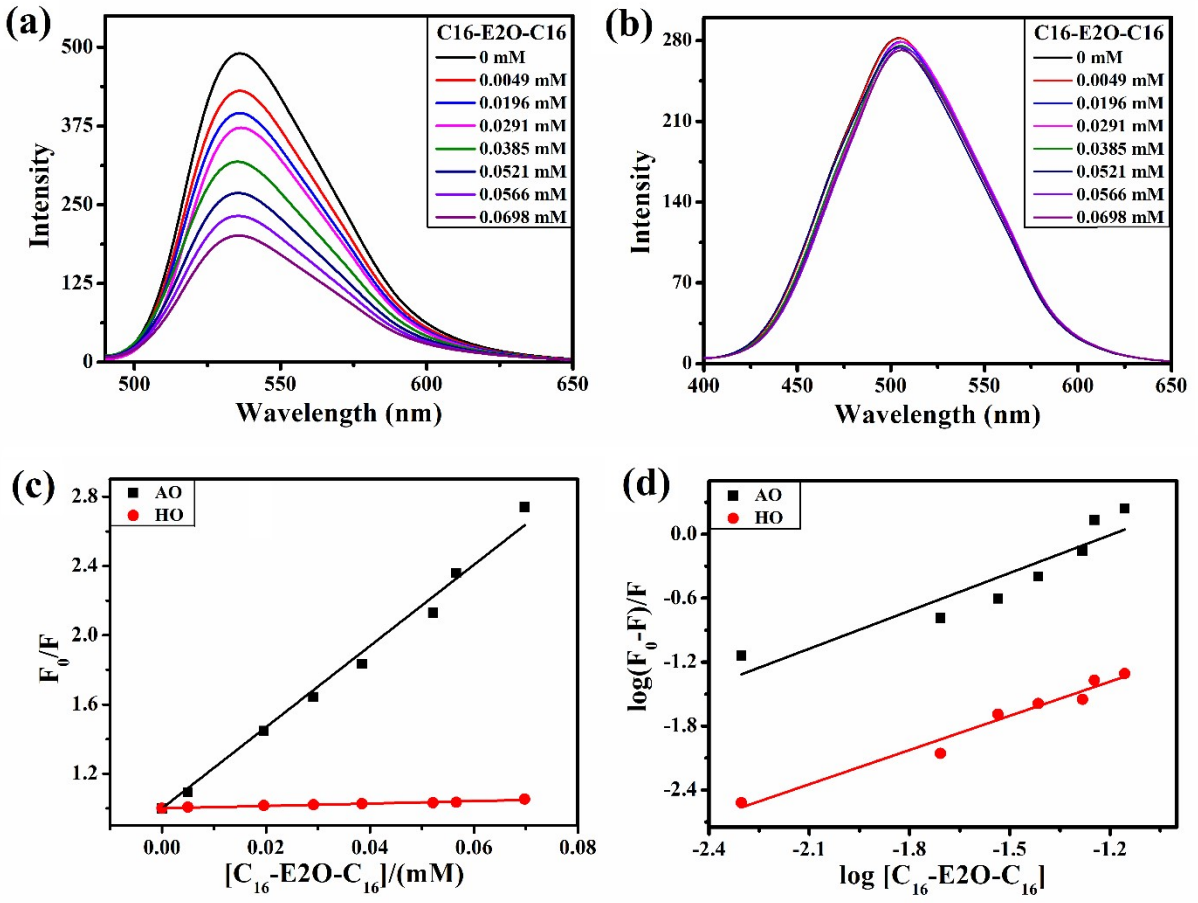

Figure S4. Competitive displacement assays between C_{16}-E2O-C_{16} gemini surfactant and dyes. Fluorescence titration of (a) AO+RNA and (b) HO+RNA systems with varying concentrations of C_{16}-E2O-C_{16} gemini surfactant. The respective Stern-Volmer and modern Stern-Volmer plots are shown in plots (c) and (d) (conditions: pH = 7.4, T = 298 K).

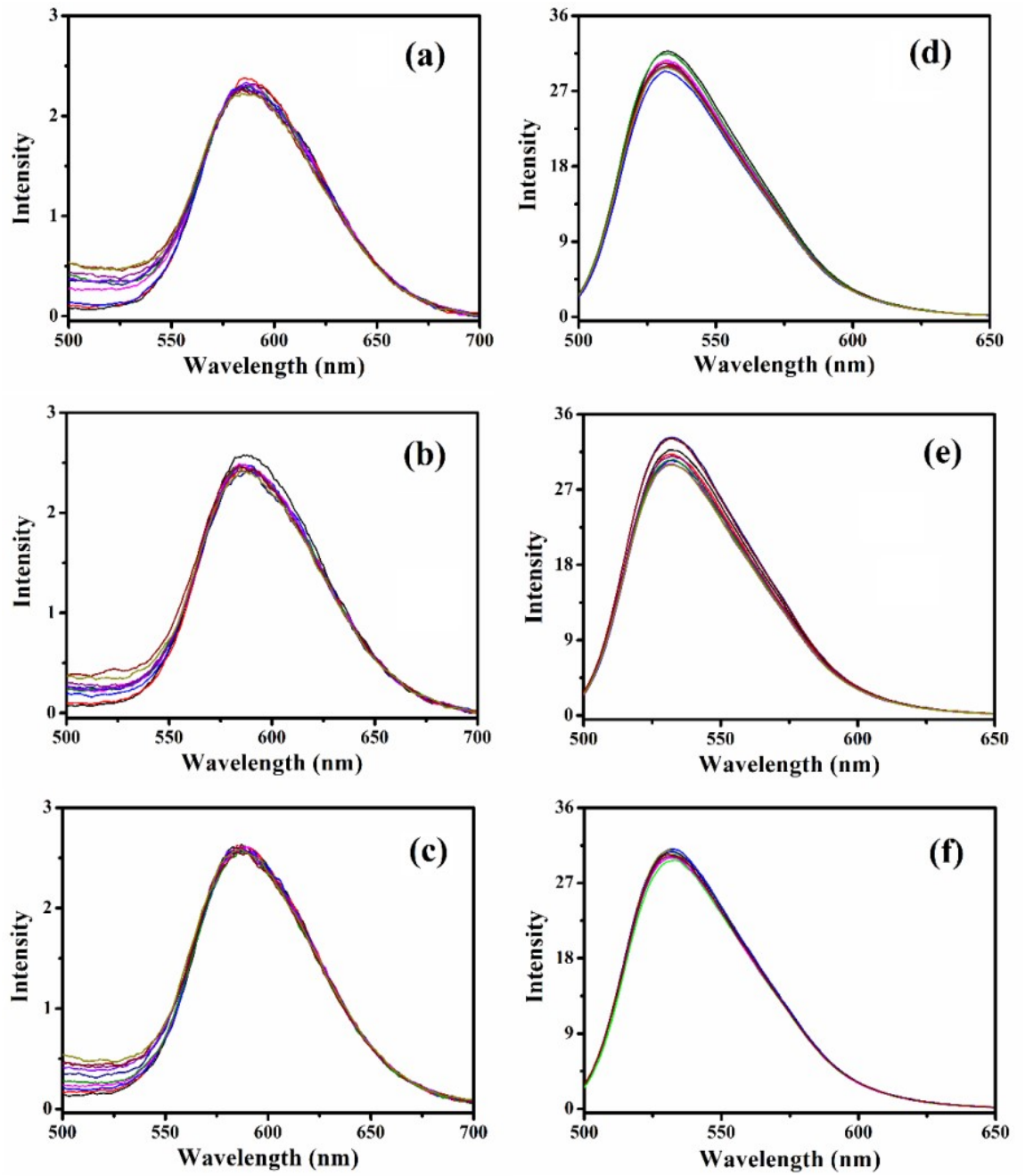

Figure S5. The fluorescence spectra of different intercalators ((a-c) ethidium bromide and (d-f) acridine orange) in the absence and presence of C_m-E2O-C_m gemini surfactants at 298 K and pH 7.4. (a & d) m=12, (b & e) m=14, (c & f) m=16.

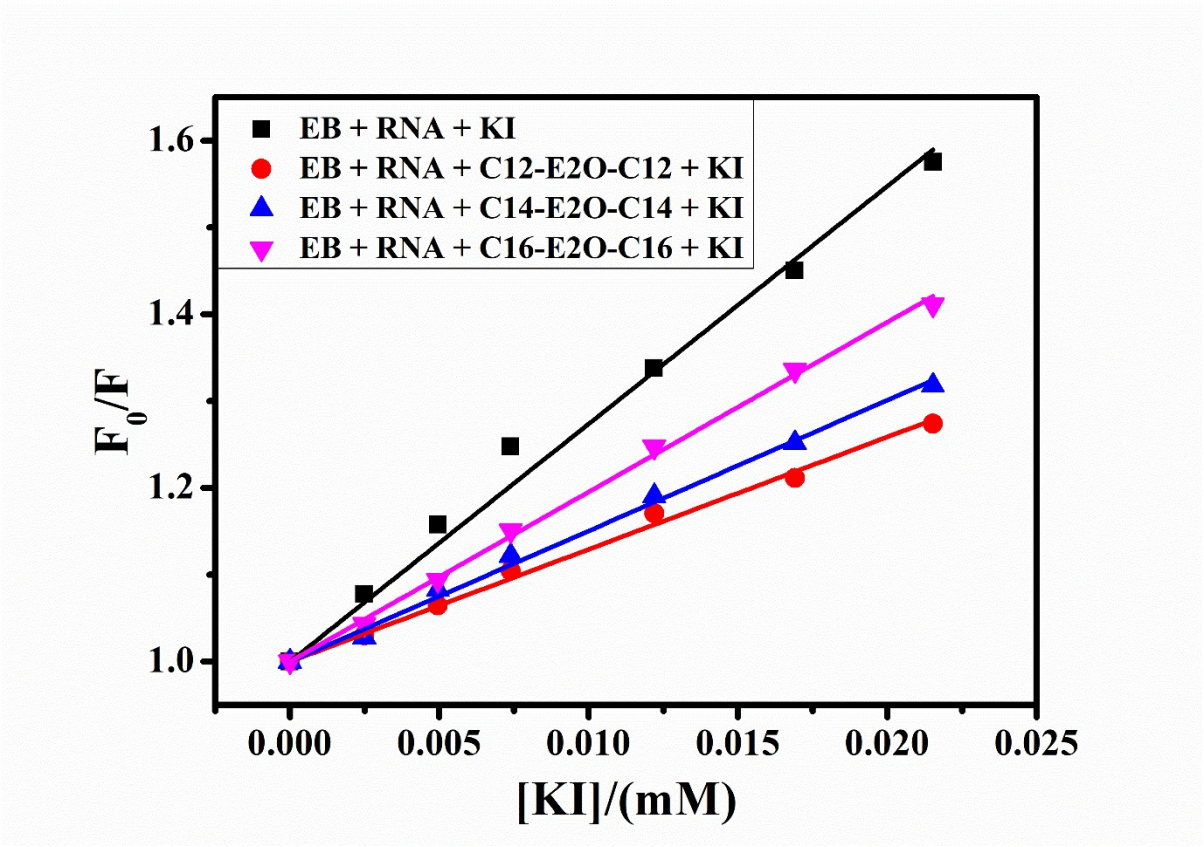

Figure S6. Stern-Volmer plots for KI quenching analysis of EB-RNA complex in the presence of C_m-E2O-C_m gemini surfactants in Tris-HCl (pH = 7.4) at 288 K.

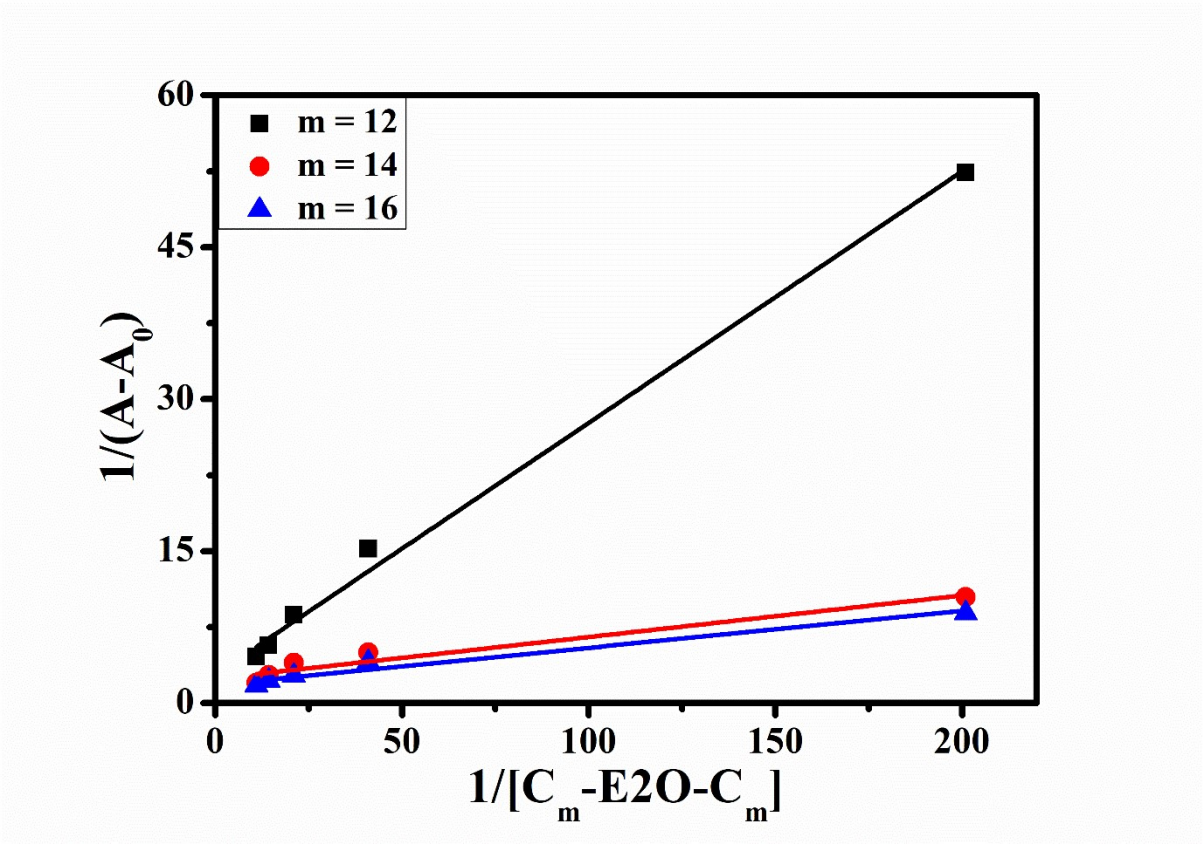

Figure S7. The double reciprocal plots of $1/(A-A_0)$ versus $1/[C_m\text{-E2O-}C_m]$ of RNA-C_m-E2O-C_m complexes (m =12, 14 and 16) at298 K and pH = 7.4 (Tris-HCl buffer).

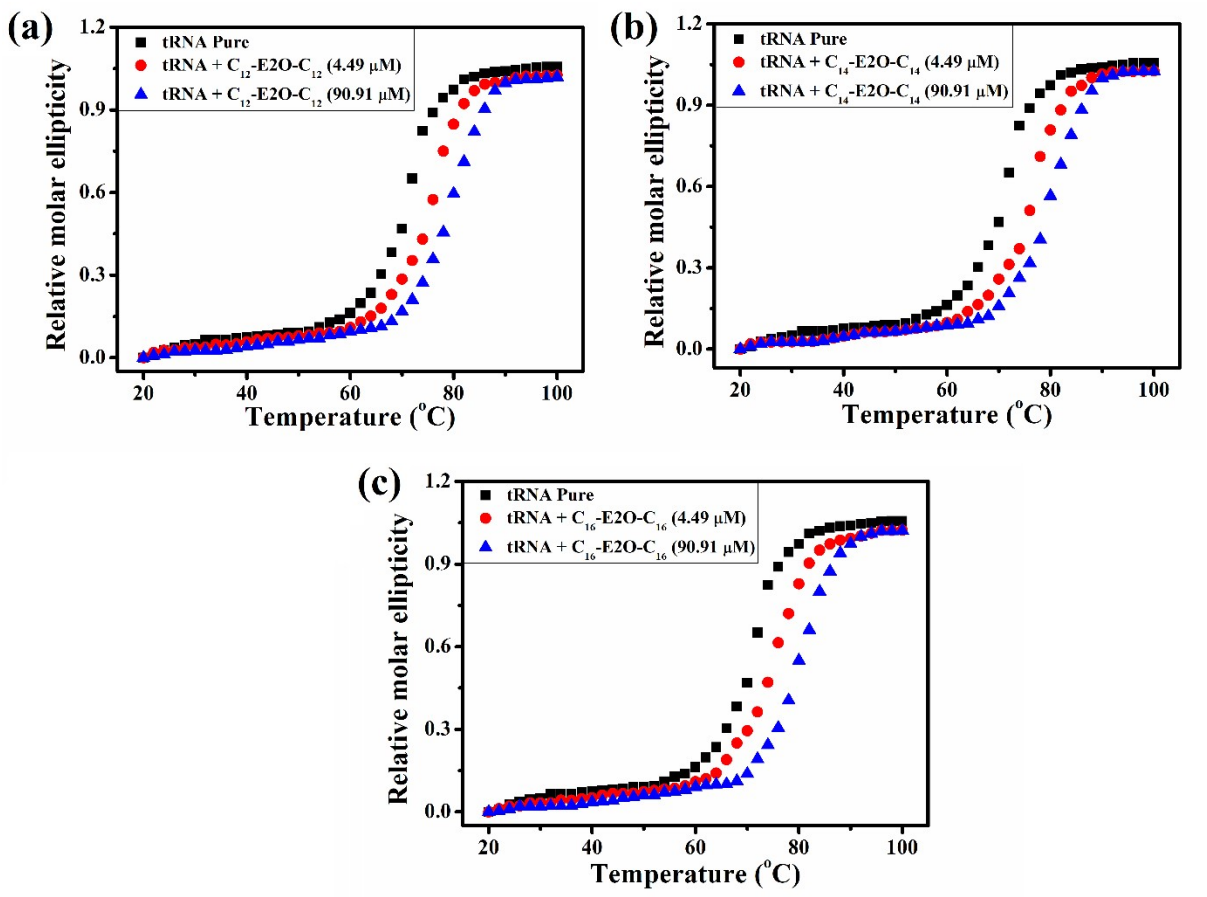

Figure S8. CD melting profiles of tRNA (5 μM) in the absence (black) and presence of (a) C_{12}-E2O-C_{12}, (b) C_{14}-E2O-C_{14}, and (c) C_{16}-E2O-C_{16} gemini surfactants (pre-(red) and post-CMC (blue)) in 100 mM Tris-HCl buffer (pH 7.4).

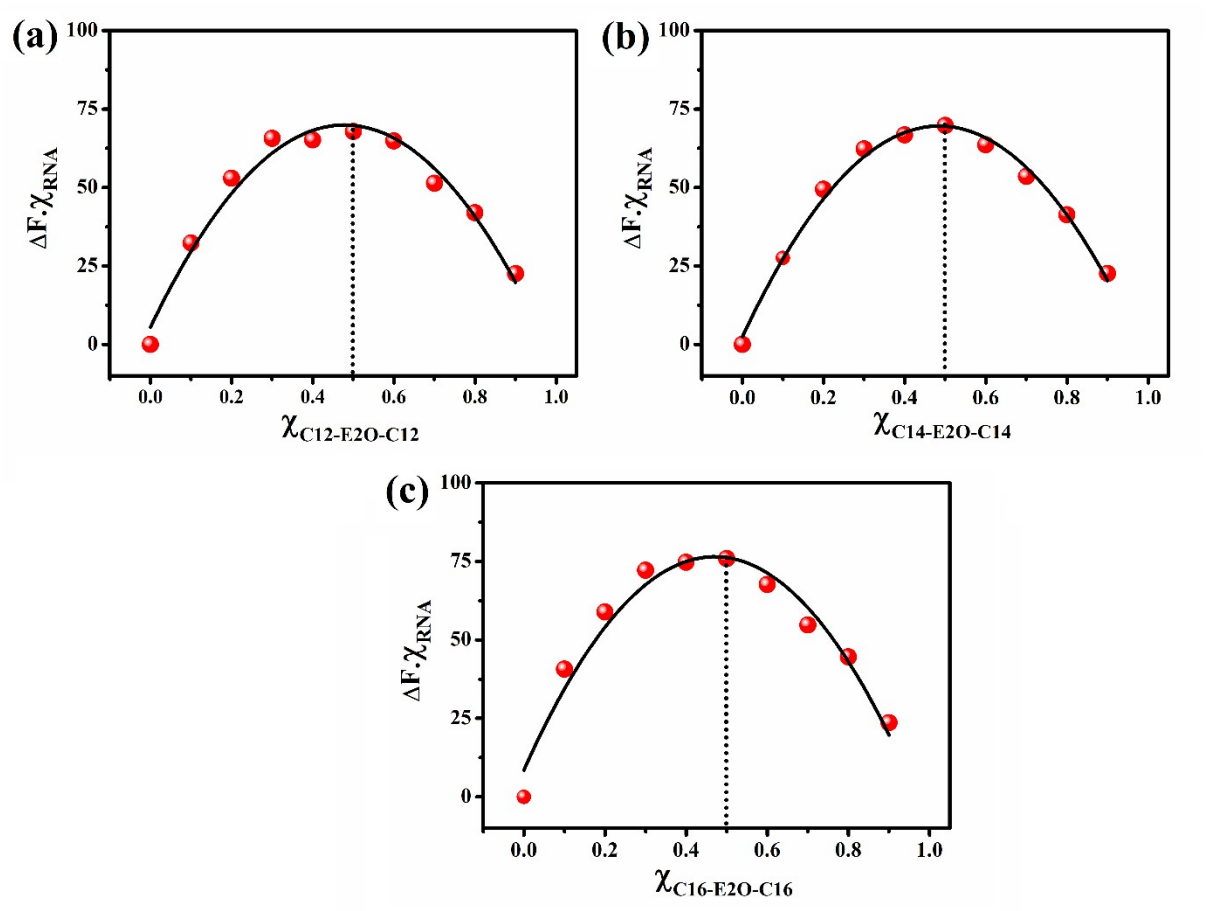

Figure S9. Job's plots for tRNA:C_m-E2O-C_m binding in Tris-HCl buffer (pH 7.4) at 298 K. The sum of the concentrations of the two components was kept constant at [tRNA]+[C_m-E2O-C_m] = 10 μM. Fluorescence emission were recorded at excitation of 473 nm.

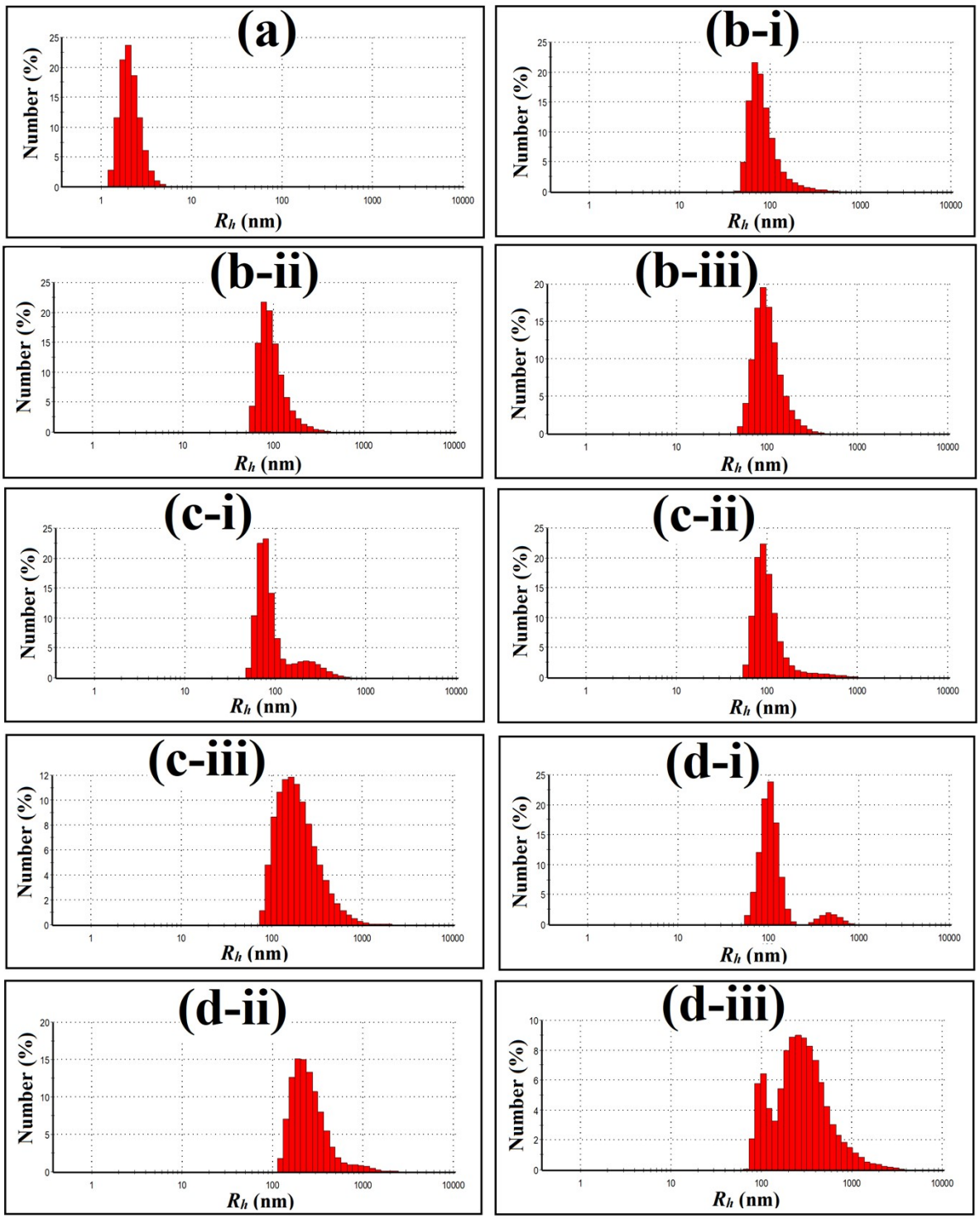

Figure S10. Dynamic light scattering results of tRNA-C_m-E2O-C_m complexes. Hydrodynamic radii (R_h) of tRNA (5 μM) in the absence (a) and presence (b-d) of C_m-E2O-C_m gemini surfactants at different concentrations ((i) = 4.96 μM, (ii) = 24.39 μM, (iii) = 47.62 μM).

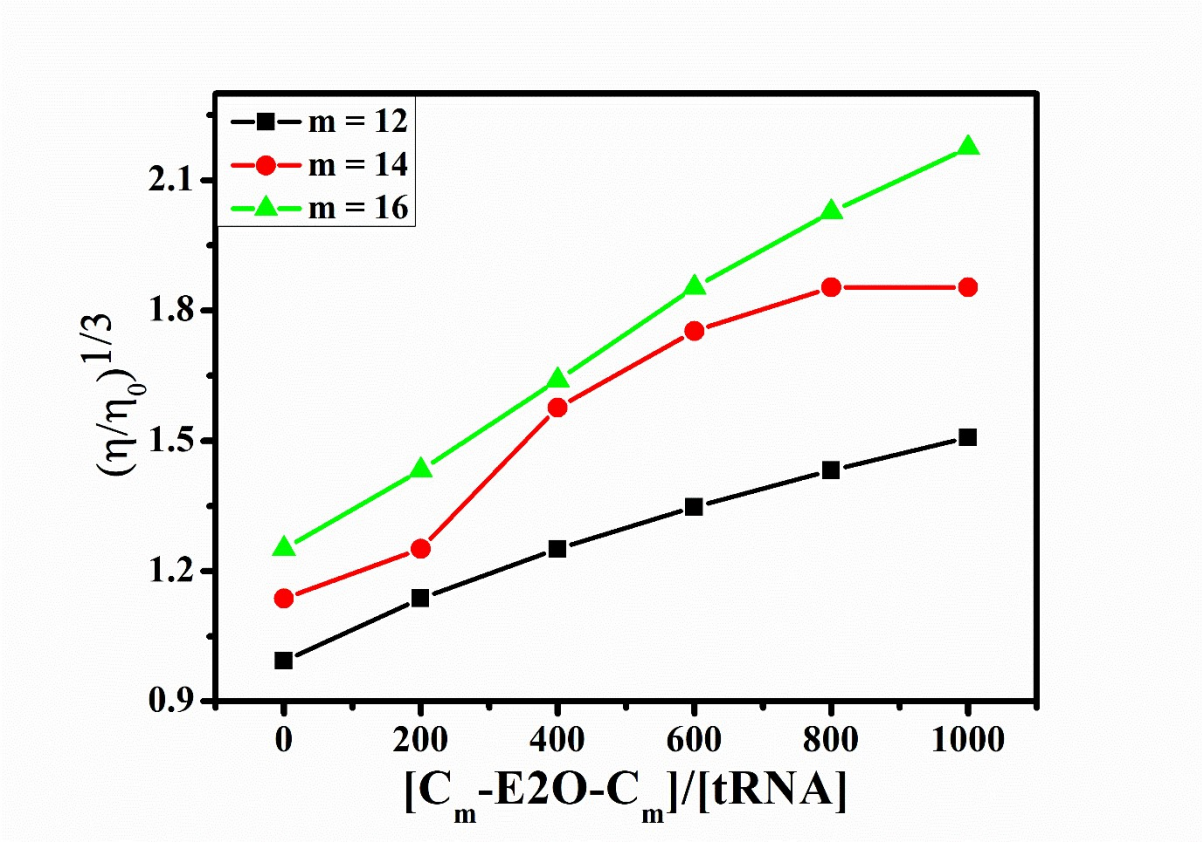

Figure S11. The viscosity graphs of tRNA at different concentrations of C_m-E2O-C_m gemini surfactants (m = 12, 14 and 16) at 298 K and pH = 7.4 (Tris-HCl buffer).

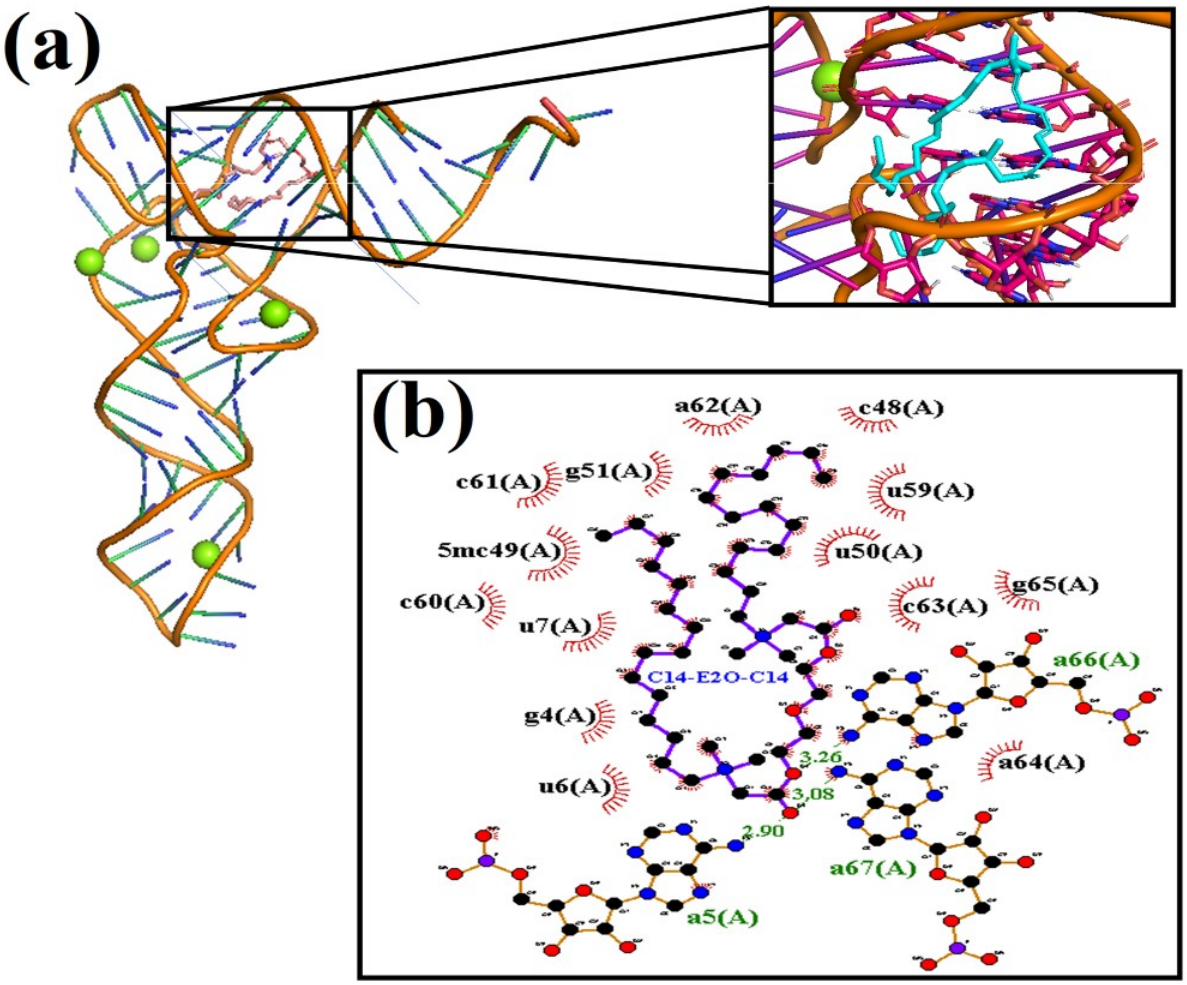

Figure S12. (a) Molecular docking view of binding of C_{14}-E2O-C_{14} gemini surfactants with tRNA, (inset) depiction of an enlarged view, and (b) 2-D view of involved molecular interactions (black color residues- hydrophobic interactions, green residues- hydrogen bonding).

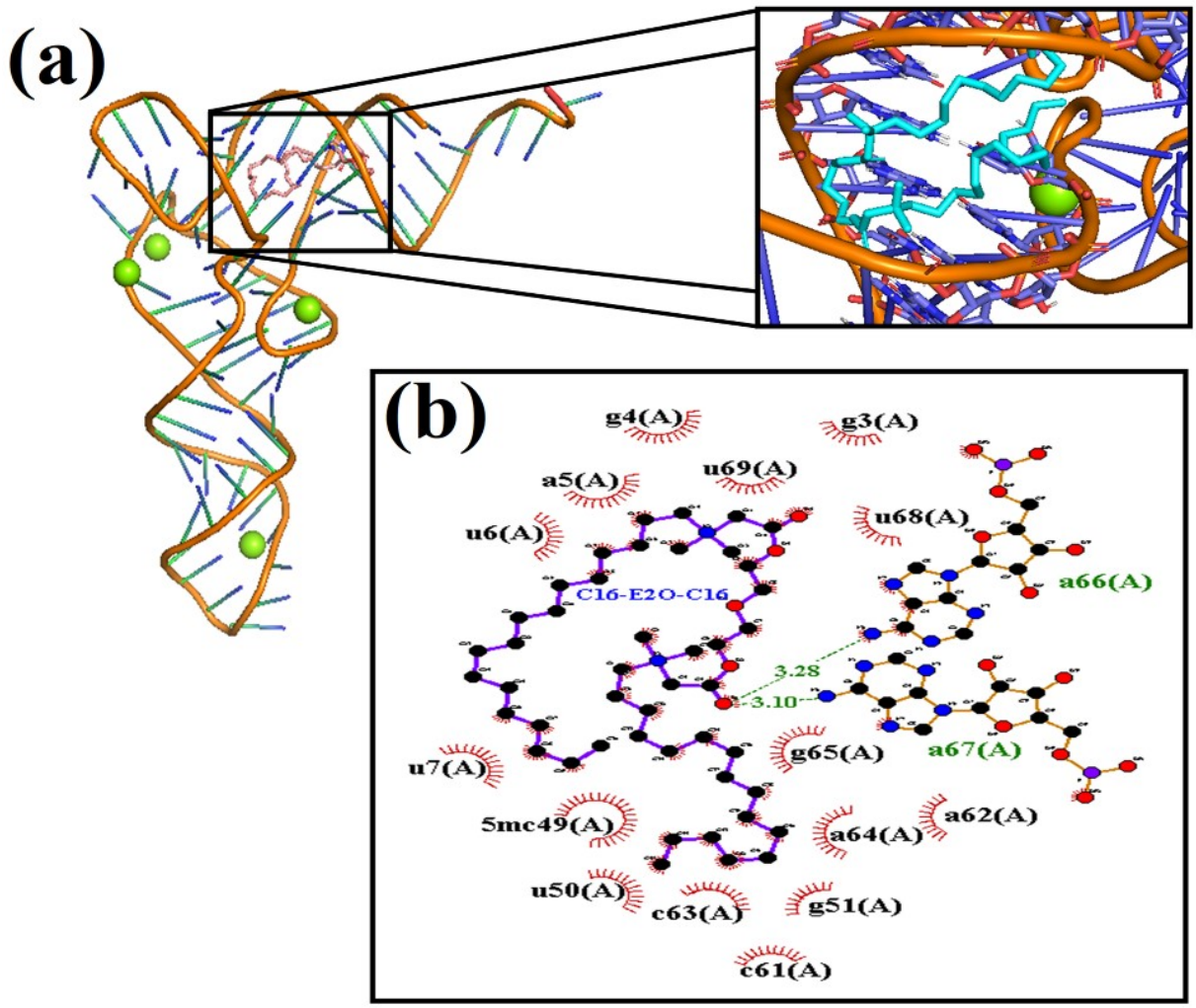

Figure S13. (a) Molecular docking view of binding of C_{16}-E2O-C_{16} gemini surfactants with tRNA, (inset) depiction of an enlarged view, and (b) 2-D view of involved molecular interactions (black color residues- hydrophobic interactions, green residues- hydrogen bonding).

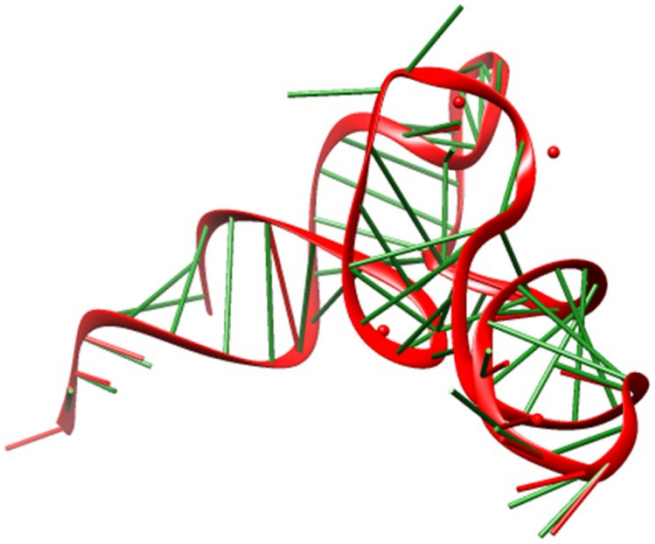

Figure S14. Superimposed structure of unbounded tRNA (red) and tRNA after simulation (green).

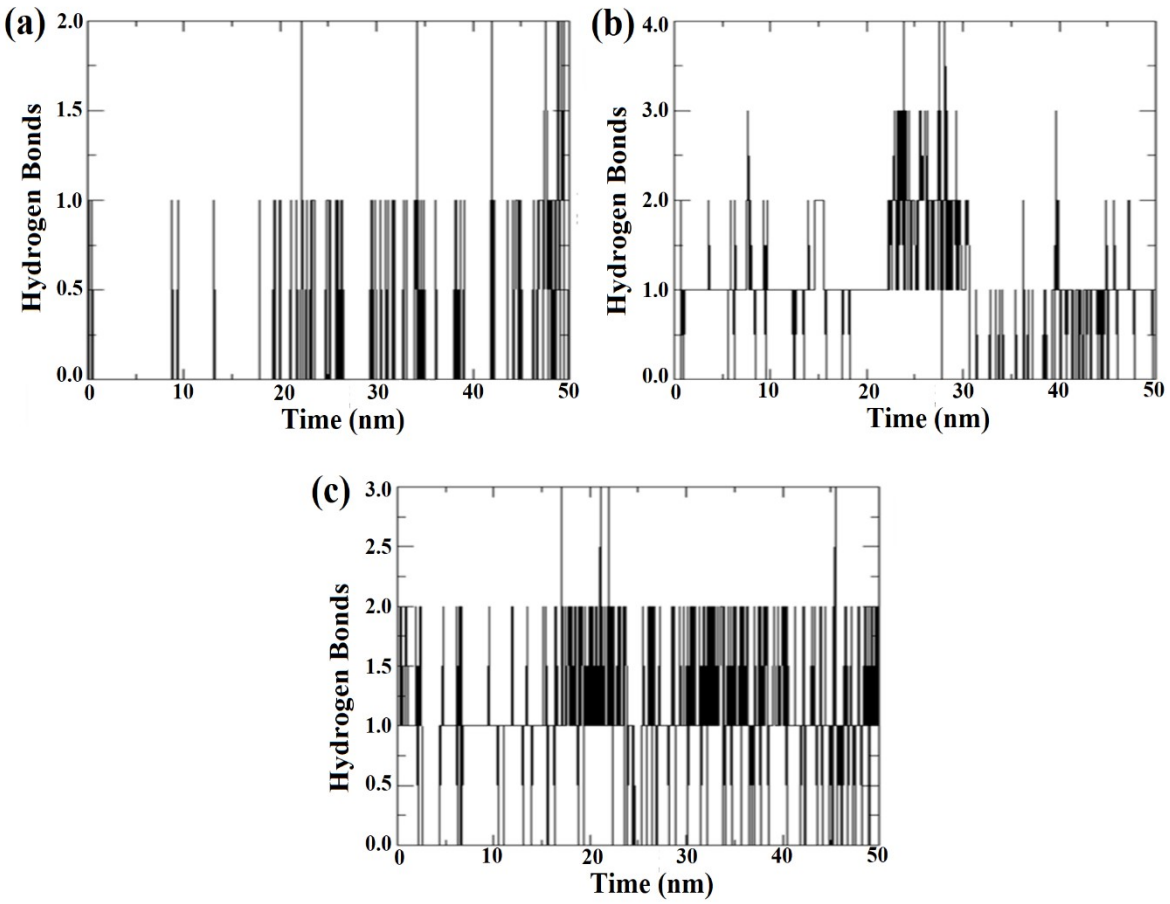

Figure S15. Number of average hydrogen bonding interactions between tRNA-C_m-E2O-C_m complexes (m = 12 (a), 14 (b) and 16 (c)) during 50 ns simulation time**.**

Table S1. Parameters obtained in KI quenching at 298 K and pH = 7.4 (Tris-HCl buffer).

Gemini Surfactant	K_{SV} ($\times 10^3$ M^{-1})	R^2
C_{12}-E2O-C_{12}	6.69	0.99
C_{14}-E2O-C_{14}	8.26	0.99
C_{16}-E2O-C_{16}	13.97	0.99

Table S2. Estimated binding constants, free energy changes and adjusted coefficients of determination for the RNA-C_m-E2O-C_m complexation from electronic absorption studies (T = 298 K, pH = 7.4).

Gemini Surfactant	K_b ($\times 10^3 M^{-1}$)	ΔG_b^0 ($kJmol^{-1}$)	R^2
C_{12}-E2O-C_{12}	11.4	-23.15	0.99
C_{14}-E2O-C_{14}	48.95	-26.75	0.97
C_{16}-E2O-C_{16}	58.59	-27.21	0.98

Table S3(a). Docking log file of RNA-C_{12}-E2O-C_{12} complex (saving top 9 orientations)

E_{min} = -5.2 kcal/mol

mode	affinity (kcal/mol)	dist from best mode rmsdl.b.	rmsdu.b.
1	-5.2	0.000	0.000
2	-5.0	6.283	11.641
3	-4.9	2.413	4.772
4	-4.8	5.912	10.260
5	-4.8	2.565	4.995
6	-4.7	6.066	10.548
7	-4.7	2.441	8.220
8	-4.7	36.554	41.526
9	-4.7	5.936	10.408

Table S3(b). Docking log file of RNA-C_{14}-E2O-C_{14} complex (saving top 9 orientations)

E_{min} = -5.4 kcal/mol

mode	affinity (kcal/mol)	dist from best mode rmsdl.b.	rmsdu.b.
1	-5.4	0.000	0.000
2	-5.3	2.734	5.298
3	-5.2	2.093	6.465
4	-5.2	29.831	34.695
5	-5.1	2.282	6.988
6	-5.1	2.581	4.492
7	-5.1	4.429	7.676
8	-5.1	3.510	10.147
9	-5.0	3.248	8.869

Table S3(c). Docking log file of RNA-C_{16}-E2O-C_{16} complex (saving top 9 orientations)

E_{min} = -5.7 kcal/mol

Mode	affinity (kcal/mol)	dist from best mode rmsdl.b.	rmsdu.b.
1	-5.7	0.000	0.000
2	-5.5	3.247	7.575
3	-5.4	3.478	7.962
4	-5.2	5.772	9.764
5	-5.1	3.288	7.808
6	-5.1	6.171	10.185
7	-5.0	3.911	7.720
8	-5.0	4.588	8.839
9	-5.0	3.132	7.861